Design, Fabrication and Testing of Surface Micromachined CMUTs for Surface and Interface Waves

Evaldas Sapeliauskas[1], Dovydas Barauskas[1], Gailius Vanagas[1], Donatas Pelenis[1], Darius Virzonis[1]
[1]*Panevezys Faculty of Technologies and Business, Kaunas University of Technology, Daukanto 12, 35212, Panevezys, Lithuania*
e.sapeliauskas@gmail.com

***Abstract*—Interdigital CMUTs were designed and fabricated in transmit/receive pairs. Each transmitter or receiver has 20 double-phase finger pairs with 146 micrometer pitch and 3 millimeter aperture. The wave transmission distance between the receiver and transmitter is 9 millimeters. Devices were fabricated on the highly doped silicon wafers by the surface micromachining technology using silicon nitride as the structural material and chromium as the sacrificial material. Interface (Scholte type) waves were transmitted and received at 100 V bias and 10 V pp 10 MHz single period harmonic burst excitation. The wave propagation velocity in water and isopropanol were measured by the spectral analysis methods. It gave us 1380 m/s and 1125 m/s phase velocity of the Scholte waves for water and isopropanol, correspondingly. We explain these reference values as specific to the measurement conditions, which are specific to our measurement conditions and particular CMUT assembly with the microchannel.**

***Index Terms*—Acoustic transducers; microfluidics; microelectromechanical devices.**

I. INTRODUCTION

Surface acoustic waves (SAW) are described as waves traveling along the surface of an elastic material, while the amplitude of motion of the material's particles decay exponentially with increasing depth. The interaction between the moving surface particles and any medium other than vacuum, affect significantly the amplitude, attenuation and velocity of the wave. SAW based delay lines are one of the most popular microelectromechanical devices in contemporary communications [1]. Also the SAWs are successfully employed for detection of the physical changes of the surface due the mechanical or chemical interaction, thus making it useful platform for sensor development [2], [3]. As an extension to the classical SAW understanding there are two types of interfacial waves: Stoneley waves, propagating at the interface of two elastic materials and Scholte waves, propagating at the interface of the solid and liquid [4]. The Scholte waves are particularity interesting in chemical and biological sensing, because this type of the waves can be used for detection of the physical properties of the liquid materials. Unlike the SAWs, interfacial waves are yet to find their application in the sensor products. The de facto standard of the micro-sized SAW delay lines or sensors fabrication technology is thin aluminum nitride (AlN) films, which exhibit excellent piezoelectrical properties [5]. Although this technological concept may be compatible with well-established microelectronics fabrication technologies (like CMOS), it calls for the modification of existing technology [6]. As alternative to the piezoelectric excitation and receive of the acoustic waves, capacitive micromachined ultrasound transducers (CMUT) were demonstrated to successfully excite and receive Scholte waves and work as a sensor of the liquid properties [7]. CMUTs can be fabricated with the standard CMOS technology and also are superior in terms of the mass sensing over the piezoelectric devices [8]. In this work we aimed to design, fabricate and test the interdigital (IDT) CMUT with separate two-phase transmit and receive transducers as a platform for the detection of physical changes of the solid and liquid interface. Also we made the reference measurements of the phase velocity of the Sholte waves in two reference fluids available at our lab: deionized water and isopropanol (IPA), which will be used in our later research.

II. DESIGN AND FABRICATION OF THE INTERDIGITAL CMUT

The layout of the IDTs pair is shown in the Fig. 1, where p_1 is the IDT period („pitch") and W is the finger length or the aperture. Unlike the piezoelectric IDTs, where a pair of the surface electrodes establish one finger of the transducer[8], CMUT interdigital transducers need only one surface electrode, since another one is at the bottom of the device.

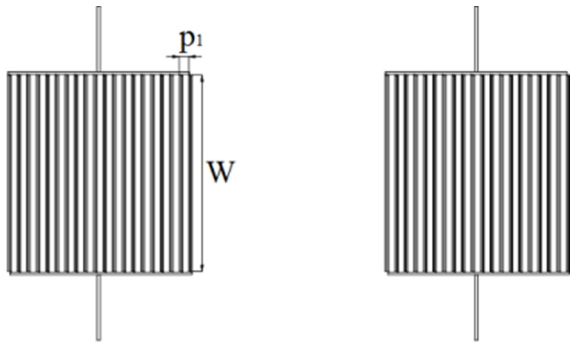

Fig. 1. Layout of the IDT pair used in this work.

Manuscript received 9 June, 2014; accepted 24 January, 2016.
This research was partially funded by a grant (No. MIP-59/2012) from the Research Council of Lithuania. Support from the European Social Fund Agency (grant No. VP1-3.1-SMM-10-V-02-024) is also appreciated.

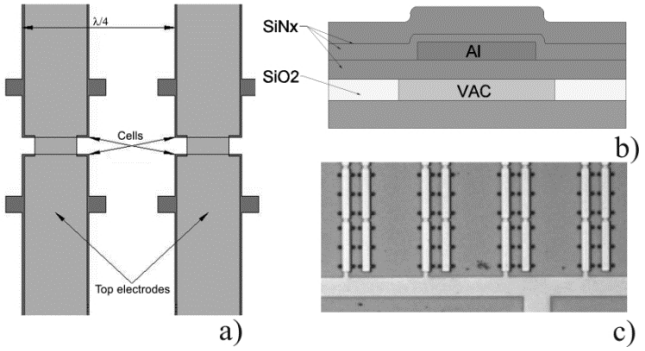

Fig. 2. Microstructure of the interdigital CMUT: a) top projection sketch of the cells; b) cross-section sketch of the single cell with; SiNx denotes silicon nitride, SiO2 – silicon dioxide, Al – alumina and VAC – vacuum; the black lines separate different silicon nitride deposition stages; c) – micrography of a part of the fabricated device. The images are not to scale.

This allows placing two sub-fingers within ¼ wavelength to enable the control over directionality of the IDT by introducing the 90° phase difference between the finger pair [9]. Both IDTs have the same number of finger pairs $N_1 = 20$. The transducer was designed for the $p_1 = 146\mu m$, which is equal to the wavelength of the Scholte wave propagating at the silicon – water interface with 1460 m/s phase velocity [10]. Design of the microstructure of the interdigital CMUT is shown on the Fig. 2. It was designed for 22 MHz air resonance at 90 V bias and corresponding 10 MHz resonance when immersed in water. Each finger of the transducer is composed of two electrically independent sub-fingers, enabling excitation of them at different phase. Sub fingers are shifted by the quarter wavelength, which is also equal to the $p_1/4 = 36.6\mu m$. Each sub-finger is composed of 16 × 100 µm CMUT cells having the same top electrode. This electrode extends over all 30 cells and connects to the bonding pads (not shown in the image) via the surface conductors at one side for the first phase and on the other side for the second phase. Overall thickness of the CMUT membrane (including 200 nm thick aluminum electrode) is 850 nm.

III. ANALYTICAL SIMULATION OF SAW

When the electrical impulse is applied to any of two phases, the diaphragms of corresponding CMUT cells deflect towards the substrate due the Coulomb interaction and snap back when the impulse ends. This transitional process also deforms the surrounding surface particles, exciting the SAW this way, which are then propagating along the surface. Figure 3(a) shows the excitation of IDT by the train of the bipolar pulses expressed here as spatial impulses (delta function) observed at a fixed point, outside of IDT. The periodicity of the waveform is

$$\tau_1 = \frac{p_1}{v_s}, \tag{1}$$

where v_s is the SAW velocity. According to [9], the acoustic impulse response of the IDT detected at an observation point

$$h_1^s(\mathrm{t}) = \frac{c_s w^2}{2} \sum_{n=0}^{N_1-1} (-1)^n (\mathrm{t} - L_n / V_s), \tag{2}$$

where c_s is a proportional constant corresponding to the SAW excitation efficiency

$$L_n = (n - N_1 + 1/2) p_1 / 2 + x, \tag{3}$$

where x is the distance from the IDT centre to the observation point.

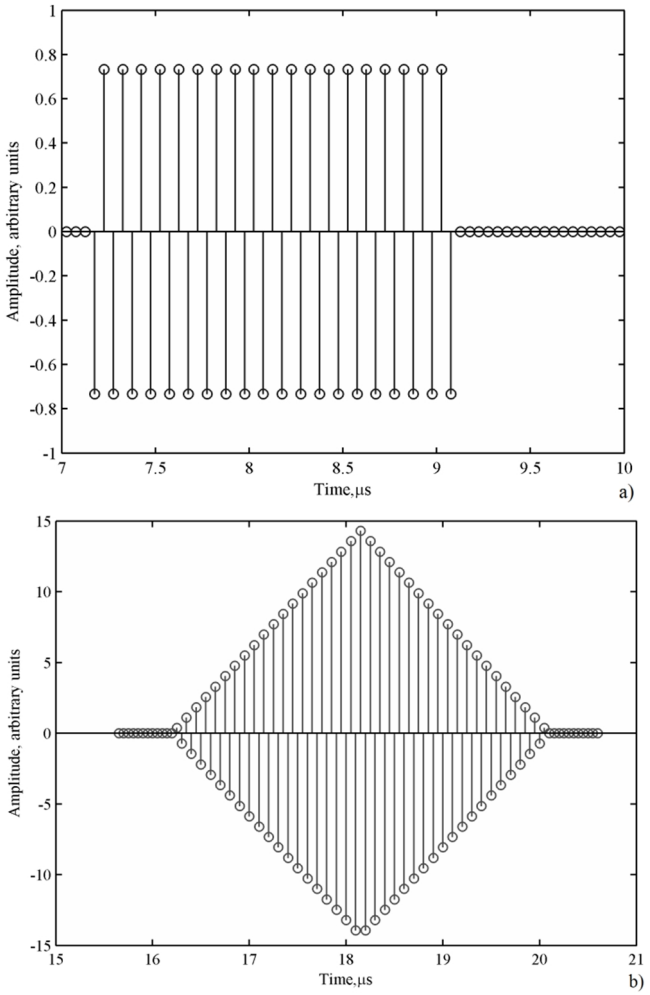

Fig. 3. Delta model of transmit pulse train of 20-finger IDT (a) and pulse train at receive 20-finger IDT side (b).

After excitation at the first IDT, a portion of the SAW energy will be received by the second IDT after a time delay. The receive pulse train can be calculated as the electrical impulse response between two IDTs (centre to centre)

$$h_{21}(\mathrm{t}) = \frac{c_s^2 w}{4} \sum_{m=0}^{2N_1-1} \sum_{n=0}^{2N_2-1} (-1)^{m+n} \delta(\mathrm{t} - L_{mn} / V_s), \tag{4}$$

where $L_{mn} = (m + n - N_1 - N_2 + 1) p_1 / 2 + L_T$, L_T here is the distance between the centres of the two IDTs and N_2 is the number of finger pairs of the second IDT. As seen from the calculated response in Fig. 3(b), number of received pulses doubles, since the transmitted pulse train first comes to the one edge, one by one pulse hitting the increasing number of fingers of the receiving IDT and exits at another edge, hitting decreasing number of receiving fingers. This cause the rhombus shaped peak-to-peak amplitude of the received pulses shown in Fig. 3(b).

IV. EXPERIMENT

The setup of the experimental system is shown in the Fig. 4. CMUT IDTs are fitted to the microchannel. One of the IDTs (2a) is connected to the two-phase transmitter (composed of two-phase arbitrary waveform generator (10, Agilent 33522A); the second IDT (2b) is connected to the two receivers (7) and oscilloscope (8, Fluke 190-502/AM). The bias source (9, Agilent N5752A) is common for both IDTs. There is also the synchronization link between the transmitter and receiver, which is not shown in the picture.

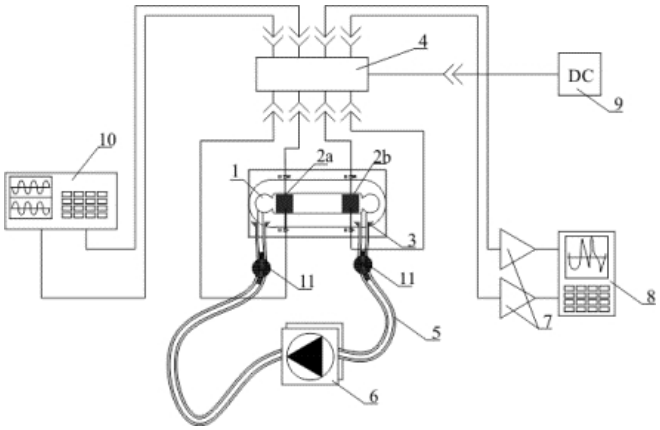

Fig. 4. Experimental setup for the interfacial waves measurement. 1 – top of the microchannel; 2a and 2b are parts of the double IDT CMUT; 3 – fluid test port; 4 – bias T; 5 – tubing; 6 – peristaltic pump; 7 – receive amplifiers; 8 – digital oscilloscope; 9 – DC bias supply; 10 - two-phase arbitrary waveform generator; 11 – fluid valves.

Such a setup is suitable for delay-line experiments for measurement of the transit time of the interfacial wave. Also, by applying the post-processing, analysis of the power spectra and phase velocity spectra was done to see the differences between the waves in different liquids. Network analyzer was used for CMUT testing.

V. CMUT FABRICATION AND TESTING

We used fully CMOS compatible surface micromachining technology approach to fabricate prototype IDT CMUTs. For the substrate and common bottom electrode we used highly doped (0.01 Ω cm), 500 µm thick 3“ silicon wafers. Prior to fabrication, wafers underwent dry oxidation to deposit 100 nm of SiO_2. This oxide layer was patterned to define 100 nm deep cavities, which then were filed with 100 nm thick sacrificial Cr layer. Then first 250 nm thick low-stress silicon nitride film was deposited by the low temperature plasma process (plasma enhanced vapor deposition, PECVD [11]). On this film 200 nm thick aluminum electrodes were deposited, patterned and protected by the second, 100 nm thick low-stresses PECVD silicon nitride film. Then the sacrificial etching vias were opened by the reactive ion etching (RIE, [12]) and the sacrificial chromium film was wet etched by the ceric ammonium nitrate based chromium etchant. After several diffusion rinsing steps the cavities were dried using critical point dryer K850WM by Quorum Technologies. Released membranes were sealed by the third, 300 nm thick low-stresses PECVD silicon nitride film, thus making the final thickness of the membrane 850 nm. Third silicon nitride film also serves as a passivation layer. The cross-section of the cell structure is shown in the Fig. 1(c). The last fabrication step is opening of the bonding pads for the bottom and top electrodes. The micrograph of the fragment of fabricated device is shown in the Fig. 1(b). After dicing the silicon chips with fabricated CMUTs were bonded to the printed circuit board, providing the conductors for the cables to solder. Wire bonding was used to interconnect the bonding pads with the printed circuit board. The interconnects were passivated by the epoxy. Microchannels were produced separately by casting the polydimethyl siloxane (PDMS) over SU8 matrix with 150 µm height profile [13]. The resulting microchannel height was 150 µm. Fabricated microchannels were cut to required shape, activated by the oxygen plasma (10 min, 100 W, 40 sccm of O_2) and glued to the silicon nitride surface. The input and output ports of the fluid was arranged using standard medicine needles. Overall picture of the CMUT and microchannel assembly is shown in Fig. 5.

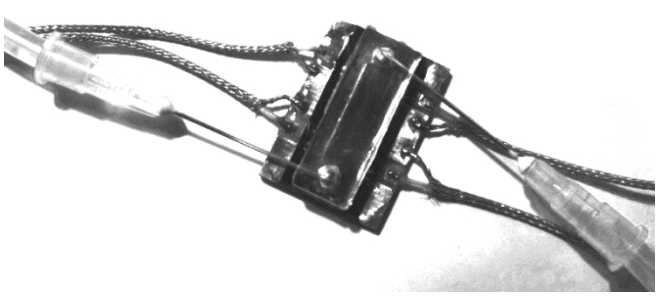

Fig. 5. CMUT IDTs and microchannel assembly.

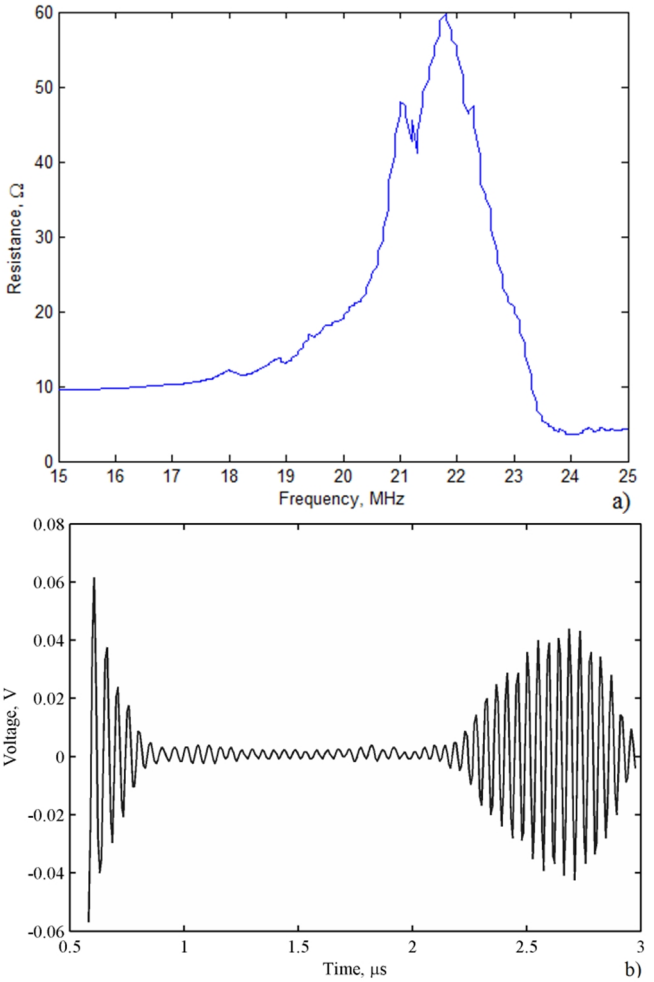

Fig. 6. Testing of the fabricated CMUT IDT: a) – frequency spectra of the real part of CMUT impedance; b) – SAW receive signal.

Fabricated and assembled CMUT IDT was tested in air, without filling the microchannel with liquid. Fig. 6(a) shows the frequency spectrum of the real part of impedance measured with the network analyser. Figure 6(b) shows the receive signal of the SAW, which was excited with the single IDT phase by 22 MHz, 5 period, 20 Vpp burst and received after delay with the second IDT. Note, this type of the wave was transmitted and received in off-resonance mode of IDT. Both these tests demonstrated the function of the measurement channel.

Immersion operation of the CMUT IDTs was tested by filling the microchannel with two different liquids: deionized water and isopropanol (IPA). The broadband excitation of the transmit IDT was used to capture the characteristic spectra of the received waves. For this we used the single-period harmonic impulse with 100 ns period and duration, with 10 Vpp amplitude. The phase velocity was calculated as a product of the measured frequency spectra of the received signal with the IDT period. The time plots of the received signals for IPA and waver are shown in Fig 7(a) and Fig 7(b). Simulated time plots are added for comparison. To simulate the delta impulses in immersion we used the same model as described in corresponding section of the current paper, except that we used approximate Scholte wave values known from the literature [7], [10]. We took the value of 1410 m/s as the Scholte wave phase velocity at silicon nitride and water interface and 1170 m/s as the Scholte wave phase velocity at silicon nitride and IPA interface. It can be seen from the phase velocity spectra of the received signals shown in Fig. 7(c) and Fig. 7(d) that measured values of the Scholte wave phase velocity are shifted towards lower frequencies from the values used in calculation. Also, since our analytical model does not take in to account attenuation and dynamical non-linearity's of the wave excitation, propagation and reception, spectra of the measured signals are wider than simulated. Also, in the case of water, the width of the measured spectrum is wider than in the case of IPA, which can be logically explained by the fact that CMUT structure is more damped by the water than IPA due the higher specific mass. This also causes lower amplitude of the received signal. From obtained data we derived new estimates of the Scholte wave phase velocity for both liquids: 1380 m/s for silicon nitride and water interface and 1125 m/s for silicon nitride and IPA interface. These estimates were taken as corresponding to the peak values of the measured spectra. We explain the differences of the new reference values from the values published in the literature by the multiple uncontrolled measurement conditions, related with CMUT and microchannel assembly that are present in our case and differ from the conditions in other labs.

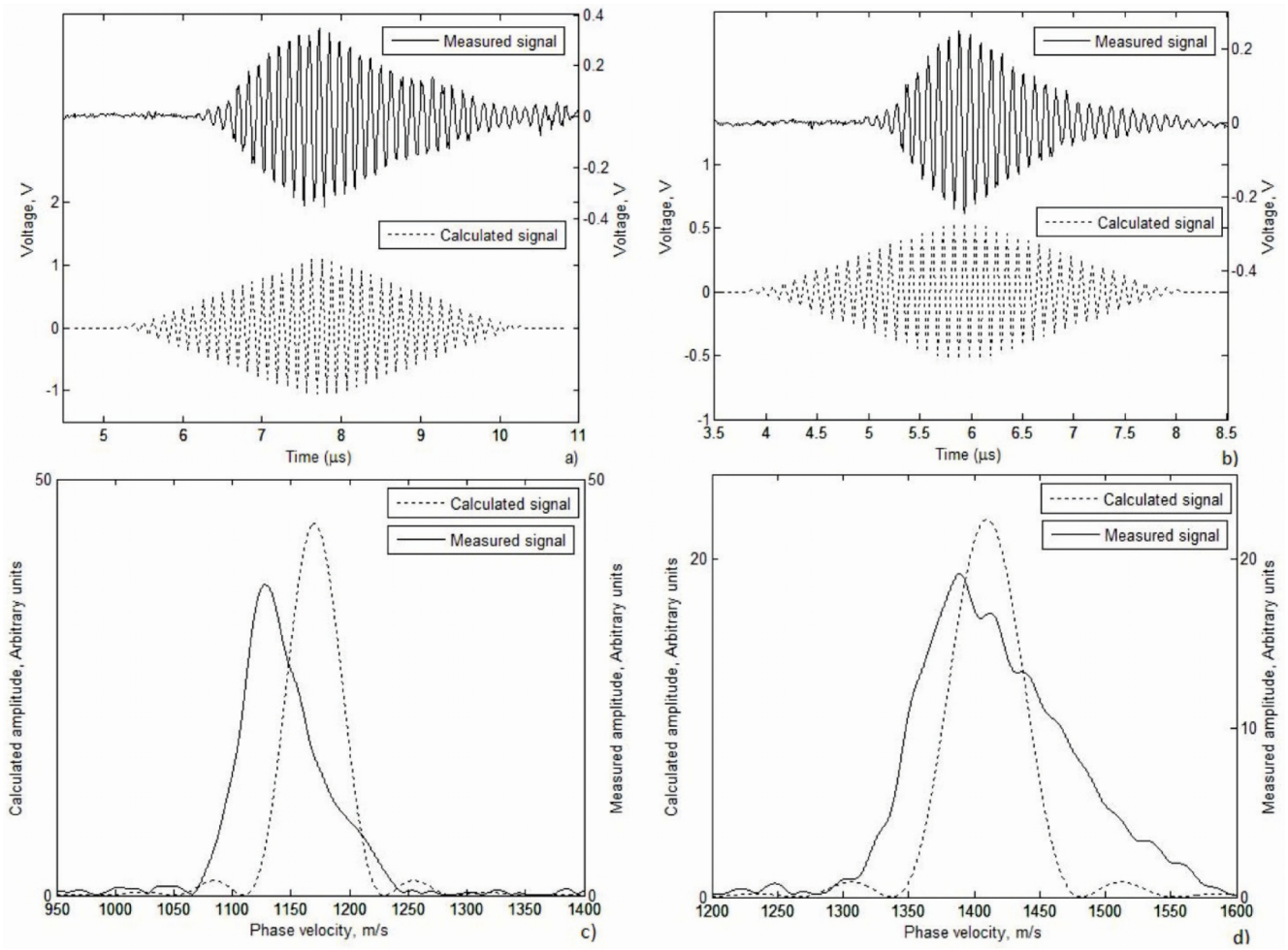

Fig. 7. Reference measurements of the Scholte wave phase velocity in fabricated CMUT IDT: a) and b) – time plots of the simulated (dashed line) and measured (continuous line) signals at receive IDT for IPA and water, correspondingly; c) and d) – spectra of the Sholte wave phase velocity, for IPA and water, correspondingly; dashed line shows simulated, and continuous line shows measured values.

VI. CONCLUSIONS

We have designed, fabricated and tested interdigital CMUTs dedicated for time of flight and/or resonance liquid properties sensing in immersion while interface waves (like Scholte waves) or, potentially, another type of the waves are used as a mean to detect physical changes at the interface between the liquid and the solid body. We demonstrated that phase velocity of the Scholte waves is a handy physical value, which can be used for detection of the liquid properties or, potentially, the changes of other properties of the interface between the solid body and the liquid. Also, we made the reference measurements, which gave us corrected values of the Scholte wave propagation at the water and silicon nitride interface (1380 m/s versus 1410 m/s) and at the isopropanol and silicon nitride interface (1125 m/s versus 1170 m/s). We also hypothesize that these corrected reference values are relevant to the particular measurement conditions.

REFERENCES

[1] M. Hribsek, "Surface acoustic wave devices in communications", *Scentific Technical Review,* vol. LVIII, no. 2, p. 10, 2008.

[2] O. Tigli, M. E. Zaghloul, "Surface acoustic wave (SAW) biosensors", *53rd IEEE Int. Midwest Symposium on Circuits and Systems*, 2010, pp. 77–80. [Online]. Available: http://dx.doi.org/10.1109/mwscas.2010.5548565

[3] I. Voiculescu, A. N. Nordin, "Acoustic wave based MEMS devices for biosensing applications", *Biosensors & Bioelectronics,* vol. 33, no. 1, pp. 1–9, 2012. [Online]. Available: http://dx.doi.org/10.1016/j.bios.2011.12.041

[4] J. G. Scholte, "On the Stoneley wave equation", in *Proc. Koninklijke Nederlandse Akademie van Wetenschappen*, vol. 45, no. 1, 1942, pp. 20–25.

[5] G. Piazza, V. Felmetsger, P. Muralt, *et al.*, "Piezoelectric aluminum nitride thin films for microelectromechanical systems", *MRS Bulletin,* vol. 37, no. 11, pp. 1051–1061, 2012. [Online]. Available: http://dx.doi.org/10.1557/mrs.2012.268

[6] J. C. Doll, B. C. Petzold, B. Ninan *et al.*, "A high CMOS compatible process for aluminum nitride on titanium", pp. 1896–1899.

[7] M. Thranhardt, P. C. Eccardt, H. Mooshofer *et al.*, "A resonant CMUT sensor for fluid applications", pp. 878–883.

[8] X. C. Jin, I. Ladabaum, F. L. Degertekin *et al.*, "Recent progress in surface micromachined capacitive ultrasonic transducers", in *Proc. 5th Int. Conf. Solid-State and Integrated Circuit Technology*, 1998, pp. 880–883.

[9] K. Nakamura, *Ultrasonic transducers*. Woodhead publishing, 2012, p. 722. [Online]. Available: http://dx.doi.org/10.1533/9780857096302

[10] J. McLean, F. L. Degertekin, "Interdigital capacitive micromachined ultrasonic transducers for sensing and pumping in microfluidic applications", *12th Int. Conf. Solid Slate Sensors, ActualOS and Micmsystems*, Boston, 2003, pp. 915–918. [Online]. Available: http://dx.doi.org/10.1109/sensor.2003.1215624

[11] M. Mikolajunas, R. Kaliasas, M. Andrulevicius *et al.*, "A study of stacked PECVD silicon nitride films used for surface micromachined membranes", *Thin Solid Films,* vol. 516, no. 23, pp. 8788–8792, 2008. [Online]. Available: http://dx.doi.org/10.1016/j.tsf.2008.06.063

[12] M. Mikolajunas, J. Baltrusaitis, V. Kopustinskas *et al.*, "Plasma etching of virtually stress-free stacked silicon nitride films", *Thin Solid Films,* vol. 517, no. 19, pp. 5769–5772, 2009. [Online]. Available: http://dx.doi.org/10.1016/j.tsf.2009.03.183

[13] D. Virzonis, G. Vanagas, R. Kodzius, "Integration of capacitive micromachined ultrasound transducers to microfluidic devices", *Microfluidics: Control, Manipulation and Behavioral Applications*, 2013.